GAS-PHASE STRUCTURES AND PHOTOCHEMISTRY DETERMINED BY PIXEL IMAGING MASS SPECTROMETRY

Michael Burt[1], Jason W. L. Lee[1], Kasra Amini[1], Hansjochen Köckert[1], Claire Vallance[1], Rebecca Boll[2], Daniel Rolles[3], Tatiana Marchenko[4], Lars Christiansen[5], Rasmus R. Johansen[5], James D. Pickering[5], Yuki Kobayashi[6], Henrik Stapelfeldt[5], and Mark Brouard[1]*

[1]Department of Chemistry, University of Oxford, Oxford, United Kingdom; [2]Deutsches Elektronen-Synchrotron, Hamburg, Germany; [3]Department of Physics, Kansas State University, Manhattan, KS, United States of America; [4]Sorbonne Universités, UPMC Université Paris 06, Paris, France; [5]Aarhus University, Aarhus, Denmark; [6]University of California, Berkeley, CA, United States of America. *mark.brouard@chem.ox.ac.uk

UNIVERSITY OF OXFORD

OVERVIEW

Ion imaging applications of the Pixel Imaging Mass Spectrometry sensor are demonstrated using Coulomb explosion velocity-map imaging and recoil-frame covariance analysis.

INTRODUCTION

Velocity-map imaging (VMI) is widely used to investigate the dynamics of small molecules. In these experiments, ions created with the same kinetic energy are focused onto the same point of a position-sensitive detector.[1] Combining this method with time-of-flight mass spectrometry further allows ions to be separated by their *m/z*. For VMI, this enables the dynamics of complex molecules to be studied.

VMI has until recently been limited by conventional imaging cameras, which image one *m/z* per experimental cycle. The development of event-triggered sensors, such as the Pixel Imaging Mass Spectrometry (PImMS) camera, overcome this restriction by enabling every resolved ion to be imaged within one experiment.[2] Here we report two ion imaging applications of the PImMS sensor: Section I investigates the photodissociation dynamics of CH_2BrI using Coulomb explosion VMI, and section II combines this method with recoil-frame covariance analysis to distinguish gas-phase structural isomers. When considered together, these applications point toward the use of multi-mass VMI as a tool for imaging the evolving structures of excited molecules within an unexcited background.

METHODS

- PImMS is a monolithic sensor that records the (x,y,t) coordinates of incident photons to a precision of 12.5 ns over 50 µs.

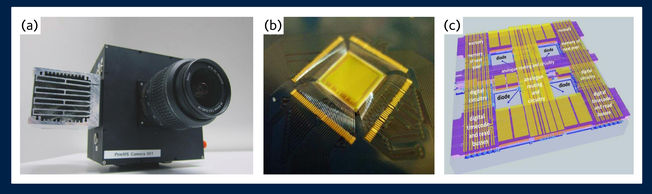

Figure 1: The PImMS camera (a), sensor (b), and sensor diagram (c).

- PImMS sensors are 72x72 (PImMS1) or 324x324 (PImMS2) pixel grids. Each pixel is 70x70 µm² and comprises four diodes measuring 14.5x14.5 µm² (Figure 1).

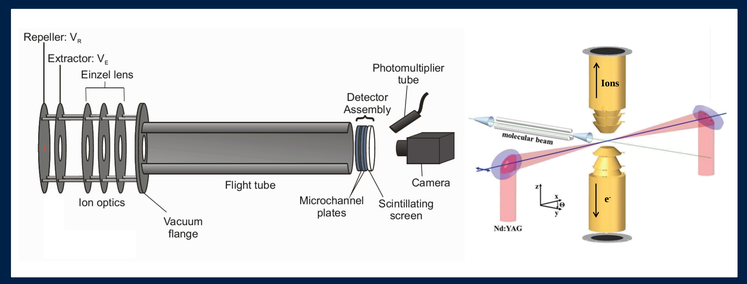

Figure 2: (left) A time-of-flight velocity-map imaging mass spectrometer. (right) The double-sided VMI instrument used in section I .

- The results presented here were acquired by coupling PImMS with conventional velocity-map imaging techniques (Figure 2). The instrument described in Section I also contained a reflected set of ion optics that allowed electrons to be velocity mapped in coincidence with ions.

I. PHOTODISSOCIATION DYNAMICS

Neutral CH_2BrI photolysis was monitored at the femtosecond scale using a time-dependent UV-IR pump-probe scheme.[3] After a set delay following UV-induced dissociation at 271 nm, field ionization at 815 nm caused the formerly neutral CH_2Br and I fragments to repel.

$$CH_2BrI \xrightarrow{h\nu_{271\,nm}} CH_2Br + I \xrightarrow{h\nu_{815\,nm}} CH_2Br^{n+} + I^{m+}$$

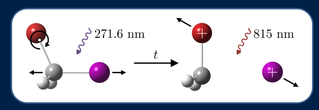

Coulomb's law dictates that the observed fragment kinetic energies depend on the distance between charge centres. The measured CH_2Br^+ and I^+ velocities therefore decreased at longer pump-probe delays (Figures 3 and 4).

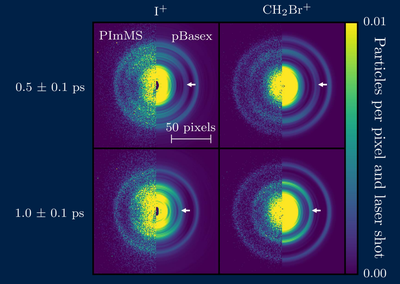

Figure 3 (left): Velocity-mapped I^+ and CH_2Br^+ images before and after pBasex Abel inversion, acquired at pump-probe delays of 0.50 ± 0.10 and 1.00 ± 0.10 ps. The arrowed rings contract with increasing delay, consistent with a Coulomb explosion occurring after neutral dissociation.

Figure 4 (below): I^+ (left) and CH_2Br^+ (right) kinetic energy distributions as a function of pump-probe delay. Projections of the 1.85 ps data are shown to the right of each figure (white lines) and compared with normalized UV (violet lines) and IR background (pink lines), as well as the sum of the asymptotic experimental data from Ref. 4 and the electrostatic kinetic energy at 1.85 ps (blue lines).

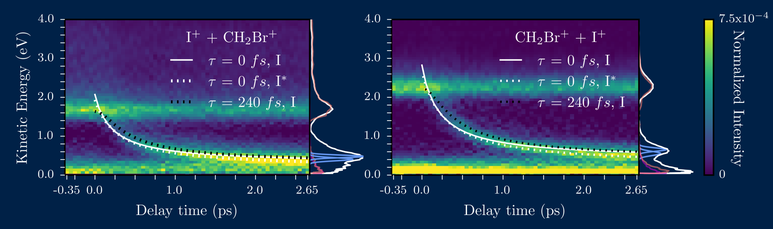

The delay-dependent kinetic energy curves correspond to CH_2BrI dissociation, and can be used to reconstruct a detailed picture of the dissociation dynamics. The following equations demonstrate that the curve shapes are sensitive to the charge location on each cofragment, the extent of ionization, and the internal excitation of the molecular fragments.

$$T_I(t-t_0) = \frac{1}{2}m_I v_I (t-t_0)^2 + \frac{k_e q_I q_{CH2Br}}{r_{IBr}(t-t_0)}\left(\frac{m_{CH2Br}}{m_I + m_{CH2Br}}\right)$$

$$T_{CH2Br}(t-t_0) = \frac{1}{2}m_{CH2Br} v_{CH2Br} (t-t_0)^2 + \frac{k_e q_I q_{CH2Br}}{r_{IBr}(t-t_0)}\left(\frac{m_I}{m_I + m_{CH2Br}}\right)$$

Fitting the experimental data to the above equations revealed the equilibrium distance $r_{IBr,eq}$ between charge centres, the fragment kinetic energies T due to UV-induced dissociation, and a phenomenological rate constant k. These are generally in excellent agreement with reference data.

Fragment	t_0 (ps)	k (ps^{-1})	$r_{IBr,eq}$ (pm)	T_I (eV)	T_{CH2Br} (eV)
I^+	0.00 ± 0.06	4.1 ± 1.6	374 ± 26	0.265 ± 0.010	0.362 ± 0.013
CH_2Br^+	-0.10 ± 0.20	2.9 ± 2.4	350 ± 80	0.244 ± 0.017	0.333 ± 0.022
Reference Data		20.8	340-350	0.25 ± 0.14	0.34 ± 0.15

II. STRUCTURAL ISOMER IDENTIFICATION

The gas-phase structures of four difluoroiodobenzene and two dihydroxybromobenzene isomers were identified by correlating the emission angles of atomic fragment ions created following femtosecond laser-induced Coulomb explosion at 800 nm.[5] The structural determinations were facilitated by confining the most polarizable axis of each molecule to the detection plane prior to their Coulomb explosion using one-dimensional laser-induced adiabatic alignment. This produced the velocity-map images shown in Figure 5. Recoil-frame covariance analysis of such ion images revealed the corresponding structural isomers (Figure 6).

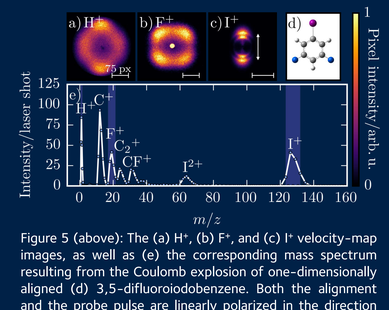

Figure 5 (above): The (a) H^+, (b) F^+, and (c) I^+ velocity-map images, as well as (e) the corresponding mass spectrum resulting from the Coulomb explosion of one-dimensionally aligned (d) 3,5-difluoroiodobenzene. Both the alignment and the probe pulse are linearly polarized in the direction shown by the arrow in panel (c).

Figure 6 (right): Recoil-frame covariance images of (a) 3,5- ; (b) 2,4-; (c) 2,5-; and (d) 2,6-difluoroiodobenzene as well as (e) 2,5-; and (f) 2,6-dihydroxybromobenzene. Each image is labeled as cov(X^+, Y^+) for a reference ion X^+ and partner ion Y^+, and represents the velocity distribution of Y^+ with respect to the velocity of X^+ recoiling at 0°. The gray shaded areas are masked regions of autocovariance.

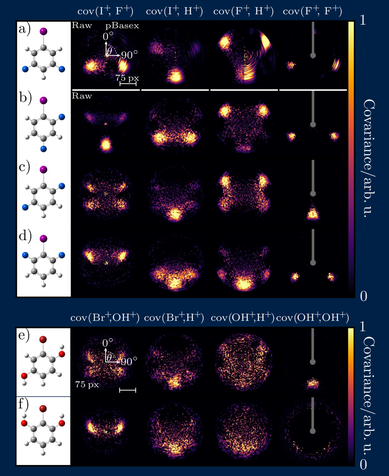

Recoil-frame covariance analysis can also distinguish structural isomers within a sample mixture (Figure 7). As mentioned previously, this could potentially allow Coulomb explosion VMI to be used as a tool to distinguish the time-dependent behaviour of excited molecules from ground-state background data.

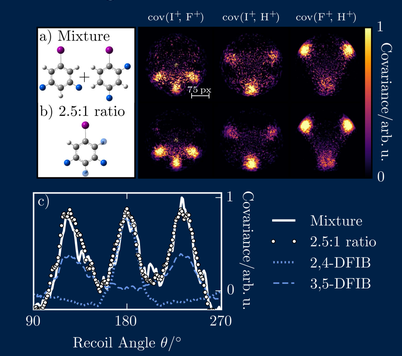

Figure 7: Recoil-frame covariance images of (a) a mixture of difluoroiodobenzene isomers and (b) the 3,5- and 2,4-isomer data in Fig. 6 summed in a 2.5:1 ratio. The labeling and representation style is the same as that used above. (c) The angular distributions of the F+ ions from the cov(I+, F+) images for the mixed sample compared with the constituent 3,5- and 2,4-DFIB isomers summed in a 2.5:1 ratio. The pictured isomer structures in (a) are added and superimposed in (b) to illustrate the overlapping molecular reference frames.

REFERENCES AND ACKNOWLEDGEMENTS

UK EPSRC funding (Grant EP/L005913/1) is gratefully acknowledged. This work is subject to a patent application by Oxford University Innovation; patent publication number US20100294924A1.

1. A. T. J. B. Eppink *et al., Rev. Sci. Instrum.*, 1997, **68**, 3477-3484.
2. J. J. John *et al., J. Instrum.*, 2012, **7**, C08001.
3. M. Burt *et al., Phys. Rev. A*, 2017, **96**, 043415.
4. L. J. Butler *et al., J. Chem. Phys.*, 1987, **86**, 2051.
5. M. Burt *et al., J. Chem. Phys.*, 2018, accepted.

Science & Technology Facilities Council
EPSRC Engineering and Physical Sciences Research Council
OXFORD UNIVERSITY INNOVATION
DESY